H-mode pedestal turbulence in DIII-D and NSTX using BOUT++ code*

X. Q. Xu[1], B. Dudson[2], E. M. Davis[3], J. W. Hughes[3], I. Joseph[1], R. J. Groebner[4], P. B. Snyder[4], R. Maingi[5], P. W. Xi[1,7] and T. Y. Xia[1,8]

[1]Lawrence Livermore National Laboratory, Livermore, California 94550 USA
[2]University of York, Heslington, York YO10 5DD, United Kingdom
[3]MIT-Plasma Science and Fusion Center, Cambridge, Massachusetts 02139, USA
[4]General Atomics, San Diego, California 92186 USA
[5]Oak Ridge National Laboratory, Oak Ridge, TN, USA
[7]School of Physics, Peking University, Beijing, China.
[8]Institute of Plasma Physics, Chinese Academy of Sciences, Hefei, Anhui 230031, China

Presented at

53rd Annual Meeting of the APS Division of Plasma Physics
November 14-18, 2011 • Salt Lake City, Utah

*This work was performed under the auspices of the U.S. Department of Energy by Lawrence Livermore National Laboratory under Contract DE-AC52-07NA27344. LLNL-PRES-513452

Abstract

In this work, we will report BOUT++ simulations for H-mode pedestal instabilities and turbulent transport. For DIII-D H-mode discharges, the BOUT++ peeling-ballooning ELM model including electron inertia was used to analyze the ideal linear stability and ELM dynamics. The beta scan is carried out from a series of self-consistent MHD equilibria generated from EFIT by varying pressure and/or current. For typical tokamak pedestal plasmas with high temperature and low collisionality, we found that the collisionless ballooning modes driven by electron inertia are unstable in the H-mode pedestal and have a lower beta threshold than ideal peeling-ballooning modes, which are the triggers for Edge Localized Modes. Thus, collisionless (electron inertia) ballooning modes might be responsible for H-mode turbulence transport when the pedestal is stable to peeling-ballooning modes. BOUT++ calculations also show that NSTX Elm stability boundaries are sensitive to flow shear profile. Attempts are underway to calculate nonlinear turbulence and transport in H-mode discharges due to the non-ideal effects.

The Nonlinear System of Equations for Simulating Non-Ideal MHD Peeling-Ballooning Modes

$$\frac{\partial \tilde{\varpi}}{\partial t} + \boldsymbol{v}_E \cdot \nabla \tilde{\varpi} = B_0 \nabla_{\|} \tilde{J}_{\|} + 2\boldsymbol{b}_0 \times \boldsymbol{\kappa}_0 \cdot \nabla \tilde{p} + \mu_{\mathrm{i},\|} \partial_{\|0}^2 \tilde{\varpi} + \mu_{\mathrm{i},\perp} \nabla_{\perp}^2 \tilde{\varpi}, \quad (1)$$

Here $\nabla_{\|} F = B\partial_{\|}(F/B)$ for any F, $\partial_{\|} = \partial_{\|0} + \tilde{b} \cdot \nabla$, $\tilde{b} = \tilde{B}/B = \nabla \tilde{A}_{\|} \times b_0/B$, $\partial_{\|0} = b_0 \cdot \nabla$, $\kappa_0 = b_0 \cdot \nabla b_0$, ion pressure P_{i} and total pressure $P = P_{\mathrm{i}} + P_{\mathrm{e}}$.

$$\frac{\partial P}{\partial t} + \boldsymbol{v}_E \cdot \nabla P = \chi_{\|} \partial_{\|0}^2 P, \quad (2)$$

$$\frac{\partial \tilde{A}_{\|}}{\partial t} = -\nabla_{\|} \Phi + \frac{\eta}{\mu_0} \nabla_{\perp}^2 \tilde{A}_{\|} - \frac{\eta_{\mathrm{H}}}{\mu_0} \nabla_{\perp}^4 \tilde{A}_{\|}, \quad (3)$$

$$\tilde{\varpi} = \frac{n_0 M_{\mathrm{i}}}{B_0} \left(\nabla_{\perp}^2 \tilde{\phi} + \frac{1}{n_0 Z_{\mathrm{i}} e} \nabla_{\perp}^2 \tilde{p}_{\mathrm{i}} \right), \qquad \Phi = \tilde{\phi} + \Phi_0,$$

$$P = \tilde{p} + P_0, \quad (4)$$

$$J_{\|} = J_{\|0} - \frac{1}{\mu_0} \nabla_{\perp}^2 \tilde{A}_{\|}, \qquad \boldsymbol{v}_E = \frac{1}{B_0} (b_0 \times \nabla_{\perp} \Phi). \quad (5)$$

This simple set of reduced two-fluid equations effectively bypasses the issue of the gyroviscous cancellations in simulations while the important diamagnetic effect is retained in the second term of the generalized vorticity expression.

Fusion Energy Sciences

The effect of transport coefficients on linear P-B instabilities.

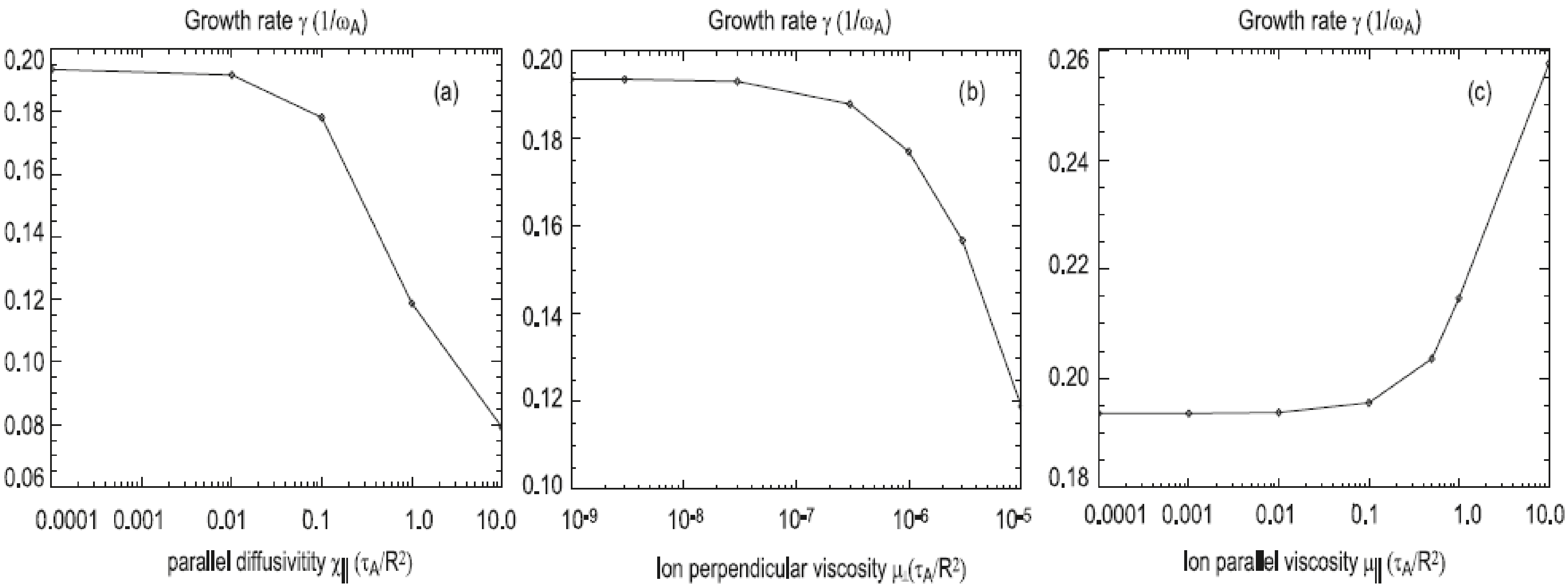

The growth rate of the $n = 15$ eigenmode versus various transport coefficients with the $E \times B$ drift and diamagnetic drift for $S = 10^8$ and $\alpha_H = 10^{-4}$: (a) the parallel diffusivity $\chi_\parallel$, (b) the ion perpendicular viscosity $\mu_{i,\perp}$ and (c) the ion parallel viscosity $\mu_{i,\parallel}$.

For ITER pedestal parameters $T_{e,ped} \simeq 4.5\,\mathrm{keV}$, $n_{e,ped} \simeq 5 \times 10^{-19}\,\mathrm{m}^{-3}$, $\chi^{SH}_{e,\parallel} \simeq 2.62 \times 10^{11}\,\mathrm{m}^2\,\mathrm{s}^{-1}$ and $\chi^{SH}_{e,\parallel}/D_A \simeq 794$, while $\chi^{FL}_{e,\parallel} \simeq v_{Te} q_{95} R \simeq 1.16 D_A$. Similarly, for typical pedestal plasma parameters, $\mu_{i\perp} \simeq (0.1-1)\,\mathrm{m}^2\,\mathrm{s}^{-1}$ as radial thermal diffusivity with the assumption that the turbulent Prandtl numbers are close to unity. Namely, $\mu_{e,\perp}/\chi_{e,\perp} \sim \mu_{i,\perp}/\chi_{i,\perp}$ and $\chi_{e,\perp} \simeq \chi_{i,\perp}$, which yields $\mu_{i\perp}/D_A \simeq (0.3\text{–}3) \times 10^{-8}$, the impact of the perpendicular ion viscosity on the growth rate is negligibly small.

Equations (1)–(5) are solved using a field-aligned (flux) coordinate system (x, y, z) with shifted radial derivatives Differencing methods used are fourth-order central differencing and third-order WENO advection scheme. The resulting difference equations are solved with a fully implicit Newton–Krylov solver: Sundials CVODE package. Radial boundary conditions used are $\tilde{\varpi} = 0$, $\nabla^2_\perp \tilde{A}_\parallel = 0$, $\partial\tilde{p}/\partial\psi = 0$ and $\partial\tilde{\phi}/\partial\psi = 0$ on the inner radial boundary; $\tilde{\varpi} = 0$, $\nabla^2_\perp \tilde{A}_\parallel = 0$, $\tilde{p} = 0$ and $\tilde{\phi} = 0$ on outer radial boundary. The domain is periodic in the parallel coordinates y (with a twist-shift condition) and in z (toroidal angle).

C-Mod Equilibrium EDA H-Mode Parameters used as BOUT++ Input (1110201023.00900)

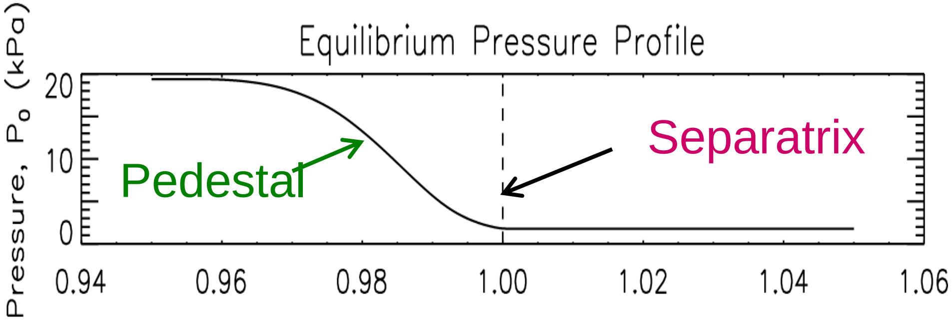

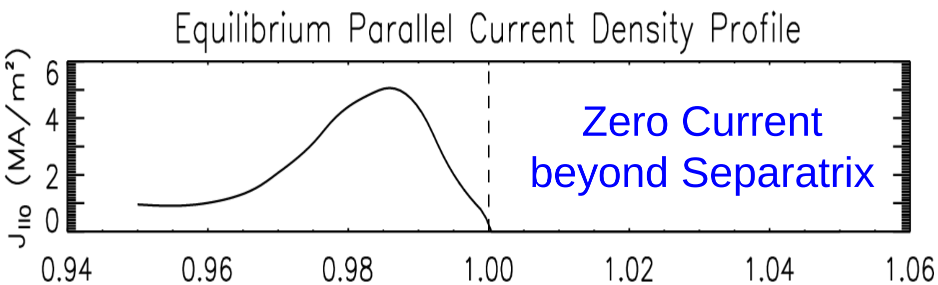

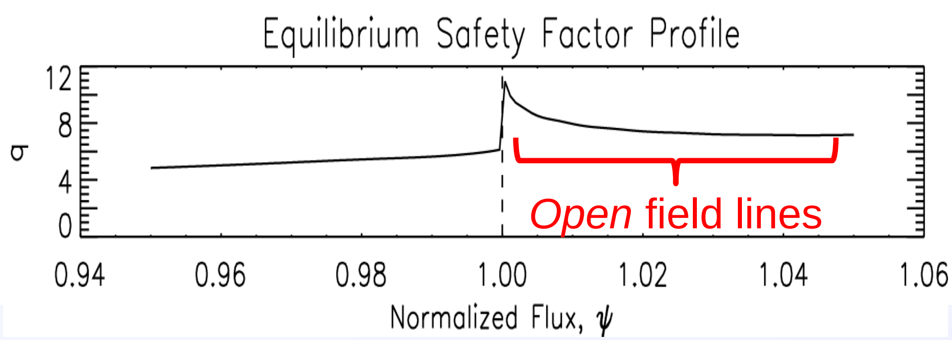

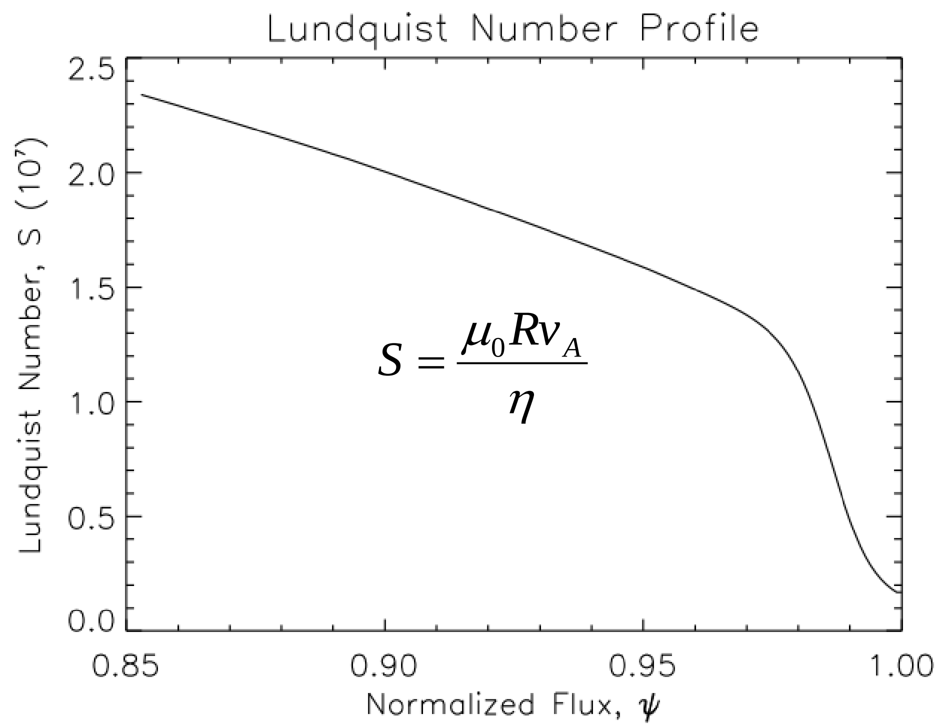

Lundquist Number (*S*) is a dimensionless ratio of the resistive diffusion time to the Alfvén time

- ***S*** **~10^7** in C-Mod EDA pedestal

Fusion Energy Sciences

Davis, et al, UP9.00008

BOUT++ Calculations Show C-Mod EDA H-Modes Resistively Unstable

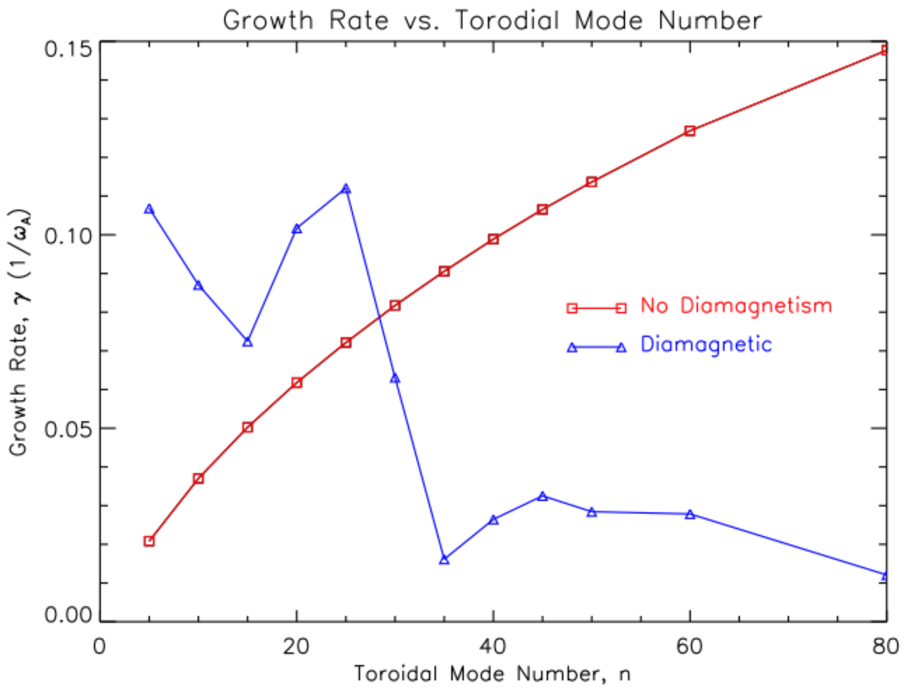

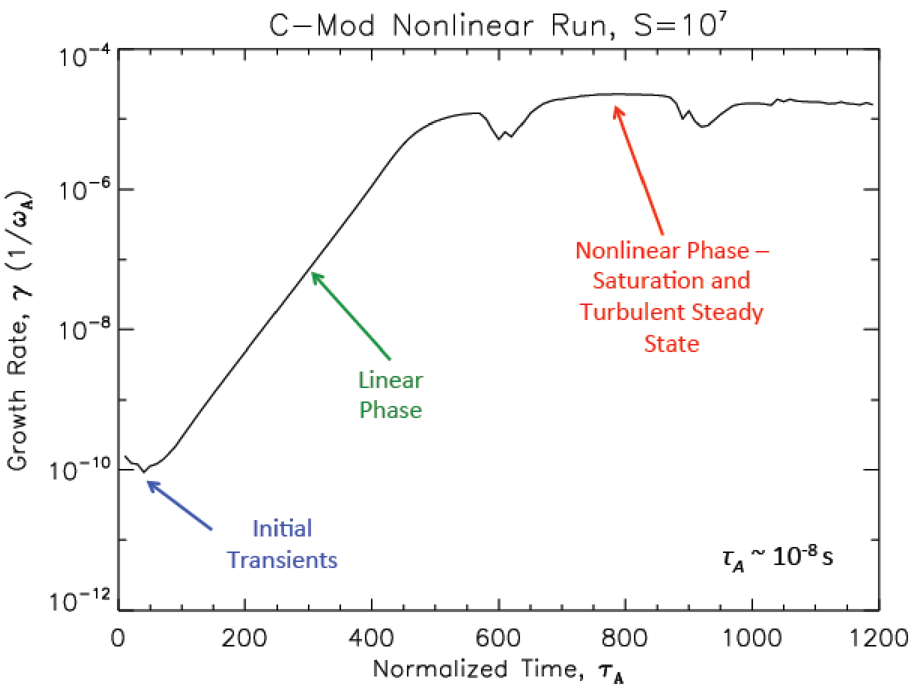

BOUT++ calculations show that Diamagnetic Effects Damp Higher Mode Numbers, yielding the growth rate peaks at n=25, consistent with measurements.

Preliminary Nonlinear Simulations have begun --- Mode Saturation and Turbulent Steady-State have been Observed. Comparisons with experimental measurements will begin.

BOUT++ simulations for DIII-D ELMy H-mode shot #131997 at reduced $J_{||}$

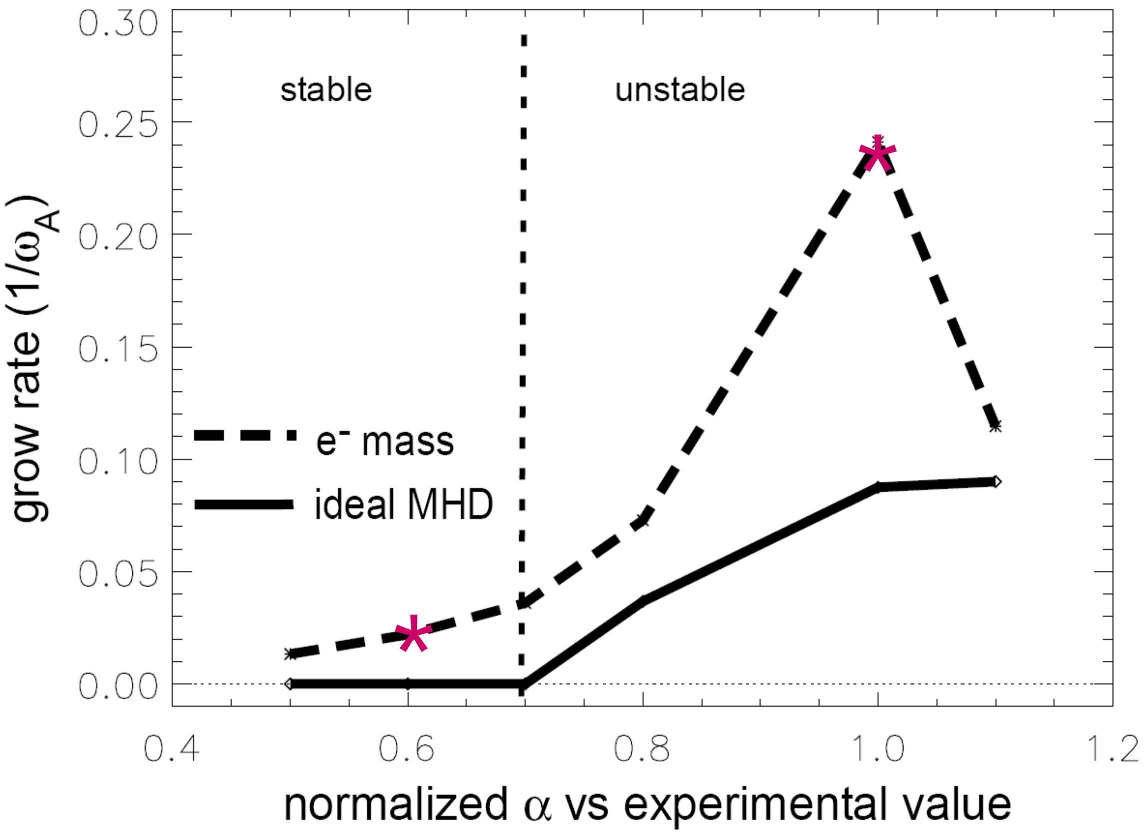

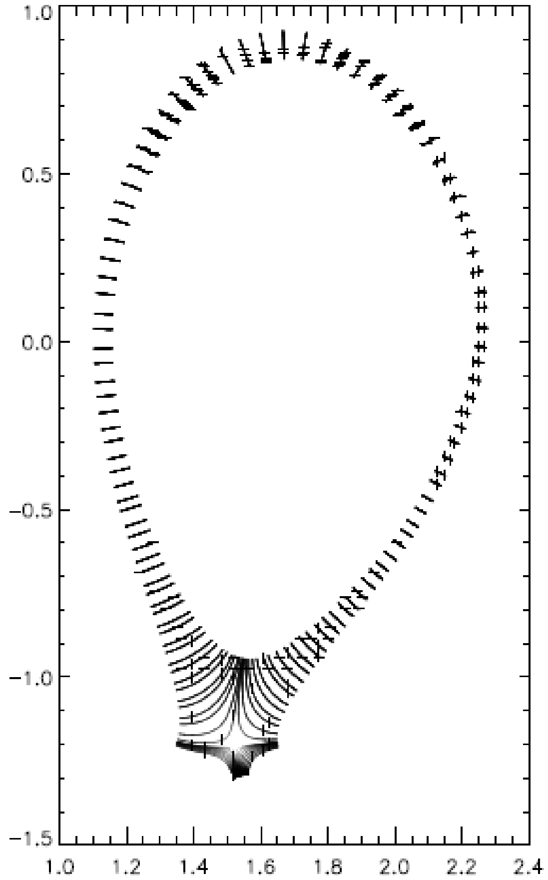

✓Ideal MHD stability boundary is consistent with infinite-n BALLOO code

✓Inclusion of e^- inertial eliminates the stability boundary

BOUT++ simulations for DIII-D ELMy H-mode shot #131997 at reduced $J_{||}$

Varyped: $P_{0,v17}=0.6P_{0,exp}$, $P_{0,v69}=P_{0,exp}$

Growth rate ($\gamma\tau_A$)

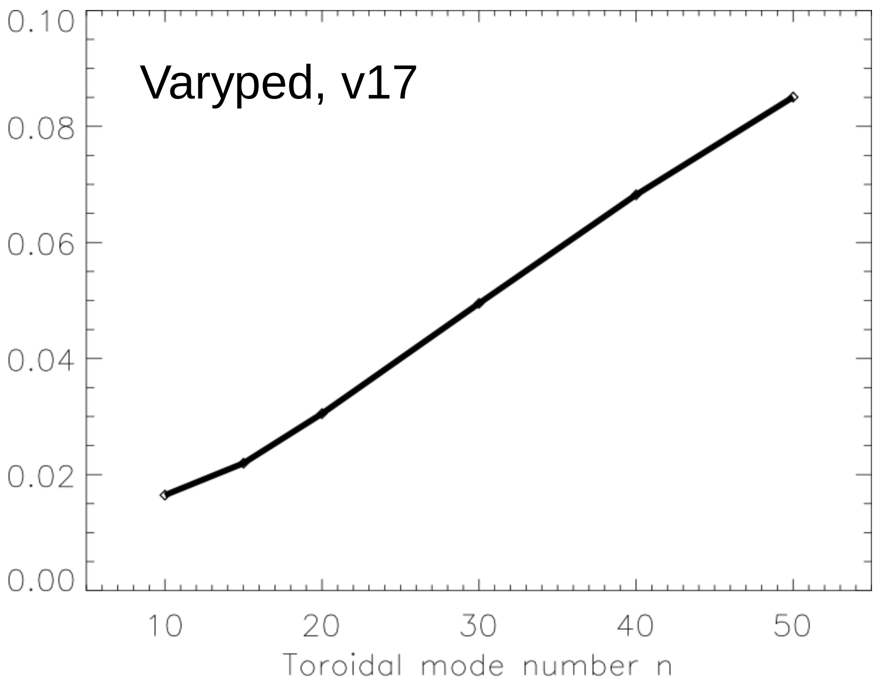

Growth rate ($\gamma\tau_A$)

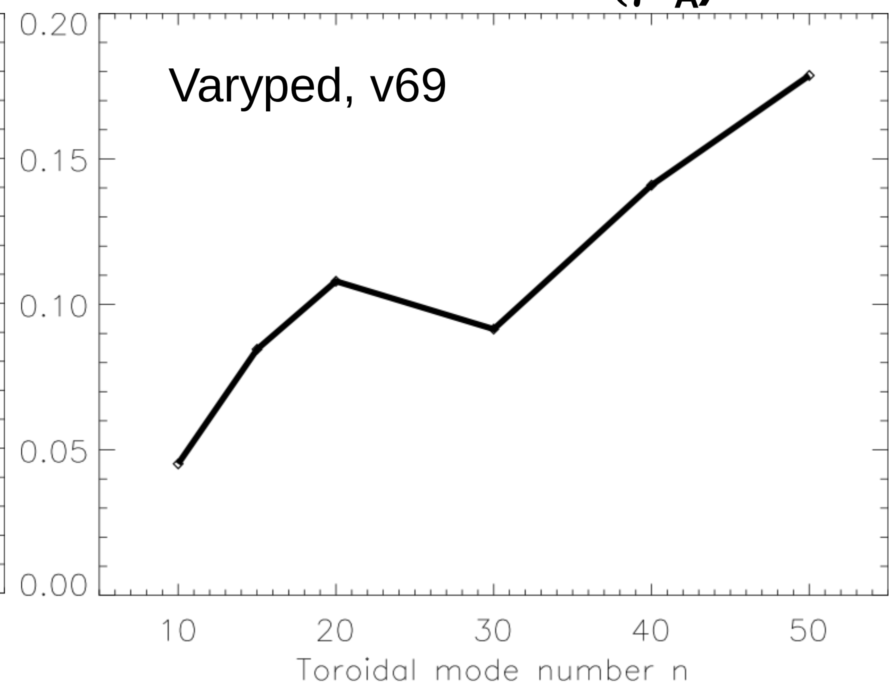

✓**Inclusion of e^- inertial eliminates or reduces the ion diamagnetic stabilization**

BOUT++ nonlinear simulations for DIII-D H-mode shot #132016 at t=3034ms & I_p=1.49MA

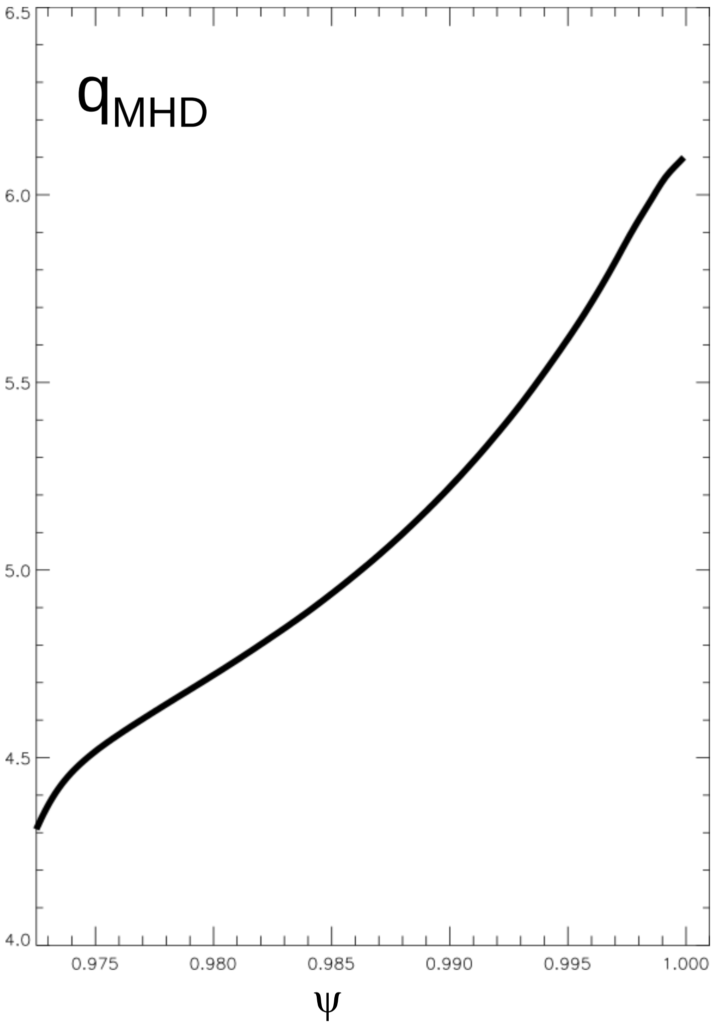

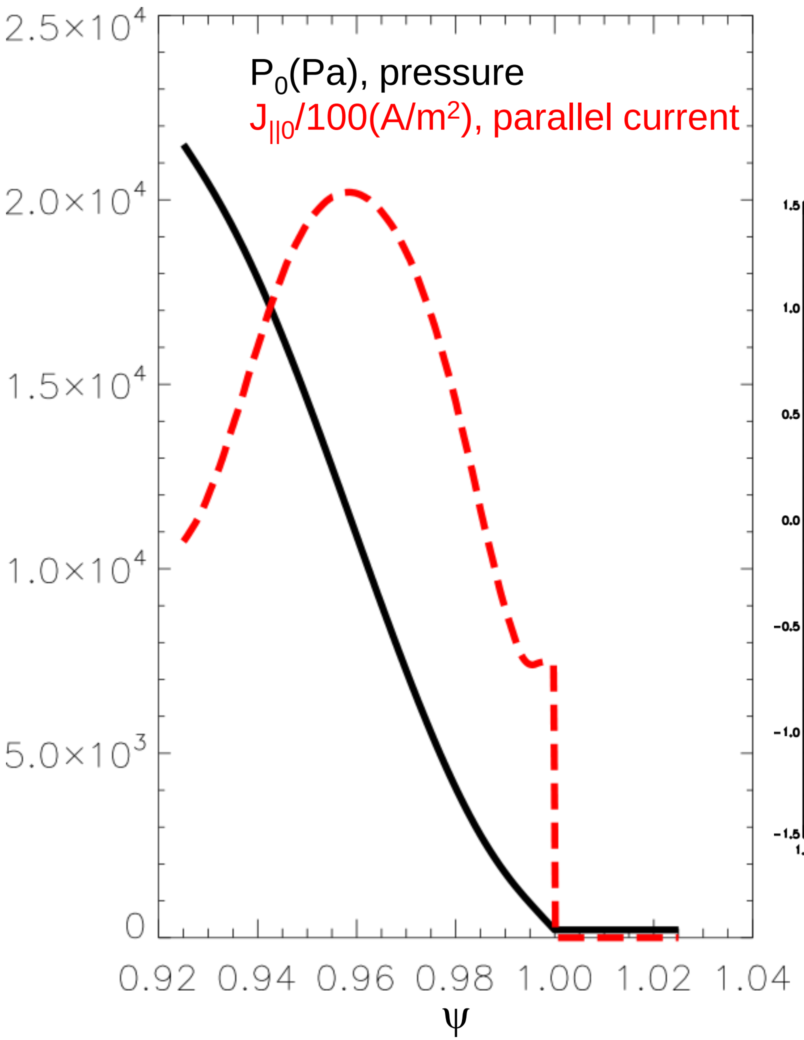

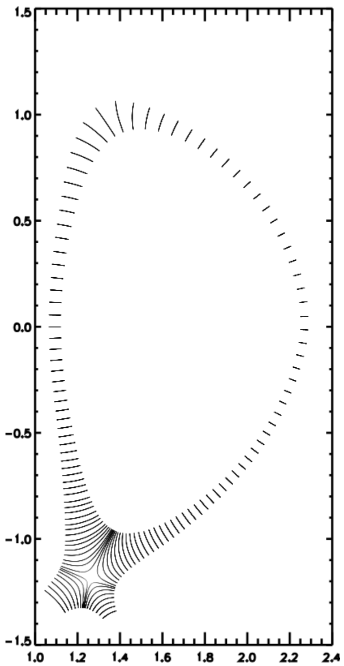

BOUT++ nonlinear simulations for DIII-D H-mode shot #132016 at t=3034ms & I_p=1.49MA

Varyped: $P_{0,v5}=P_{0,exp}$, $P_{0,v10}=1.5P_{0,exp}$

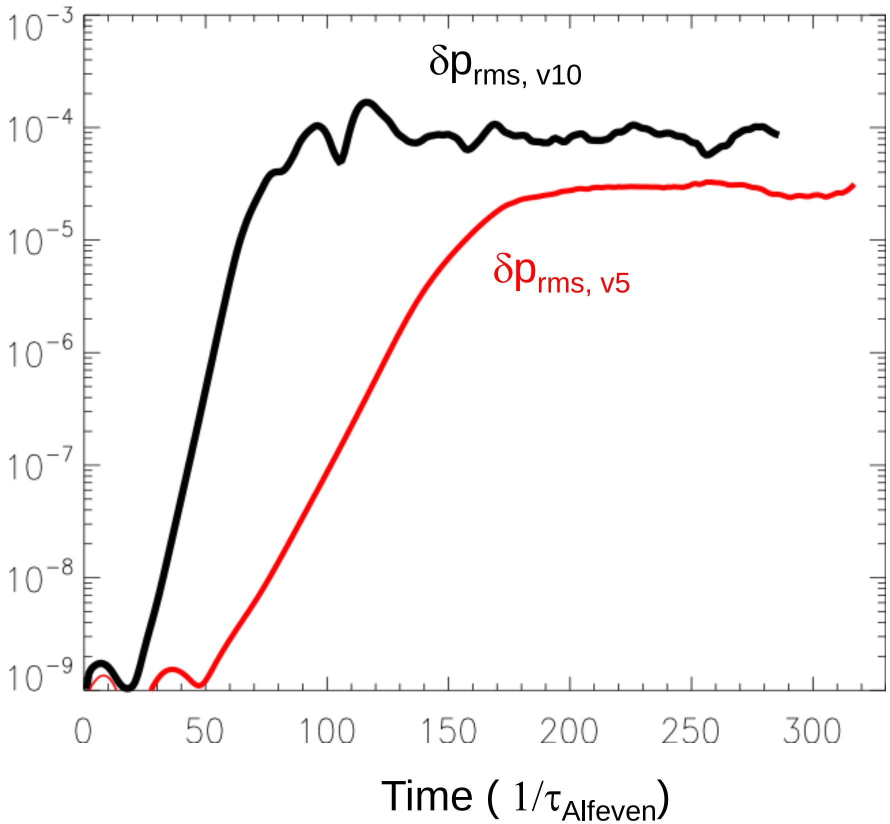

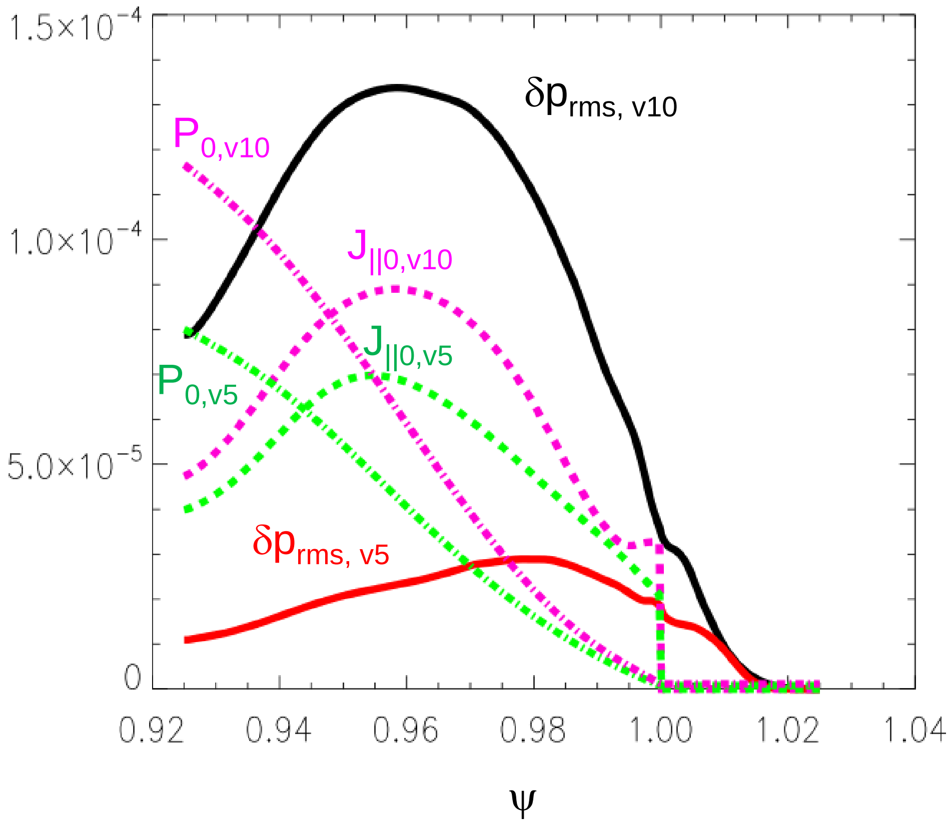

✓Inclusion of e^- inertial eliminates the stability boundary

BOUT++ nonlinear simulations for DIII-D H-mode shot #132016 at t=3034ms & I_p=1.49MA

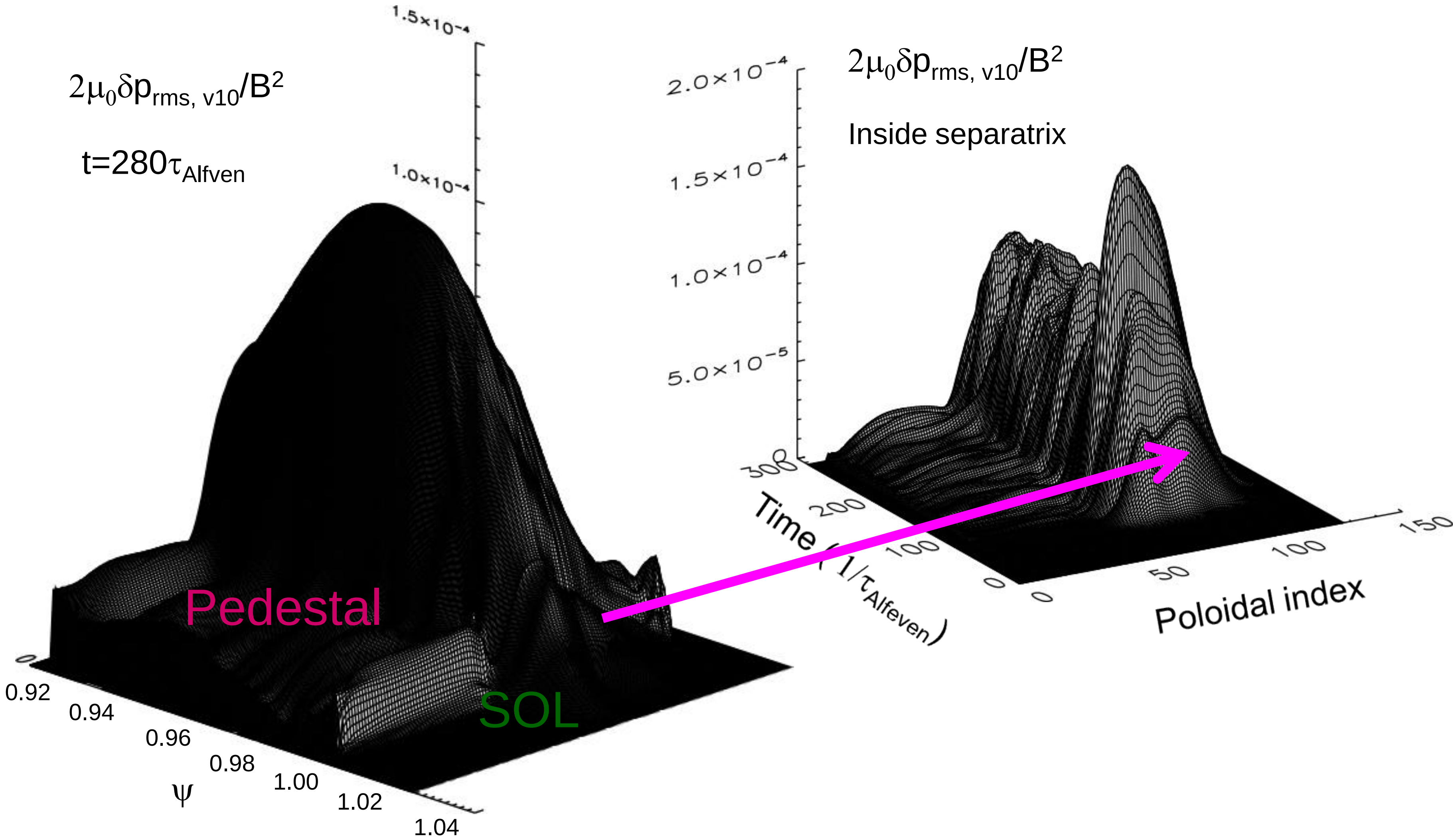

✓Keeping ballooning mode eigen-function from linear to nonlinear phase

Fusion Energy Sciences

DIII-D NATIONAL FUSION FACILITY SAN DIEGO

BOUT++ nonlinear simulations for DIII-D H-mode shot #132016 at t=3034ms & I_p=1.49MA

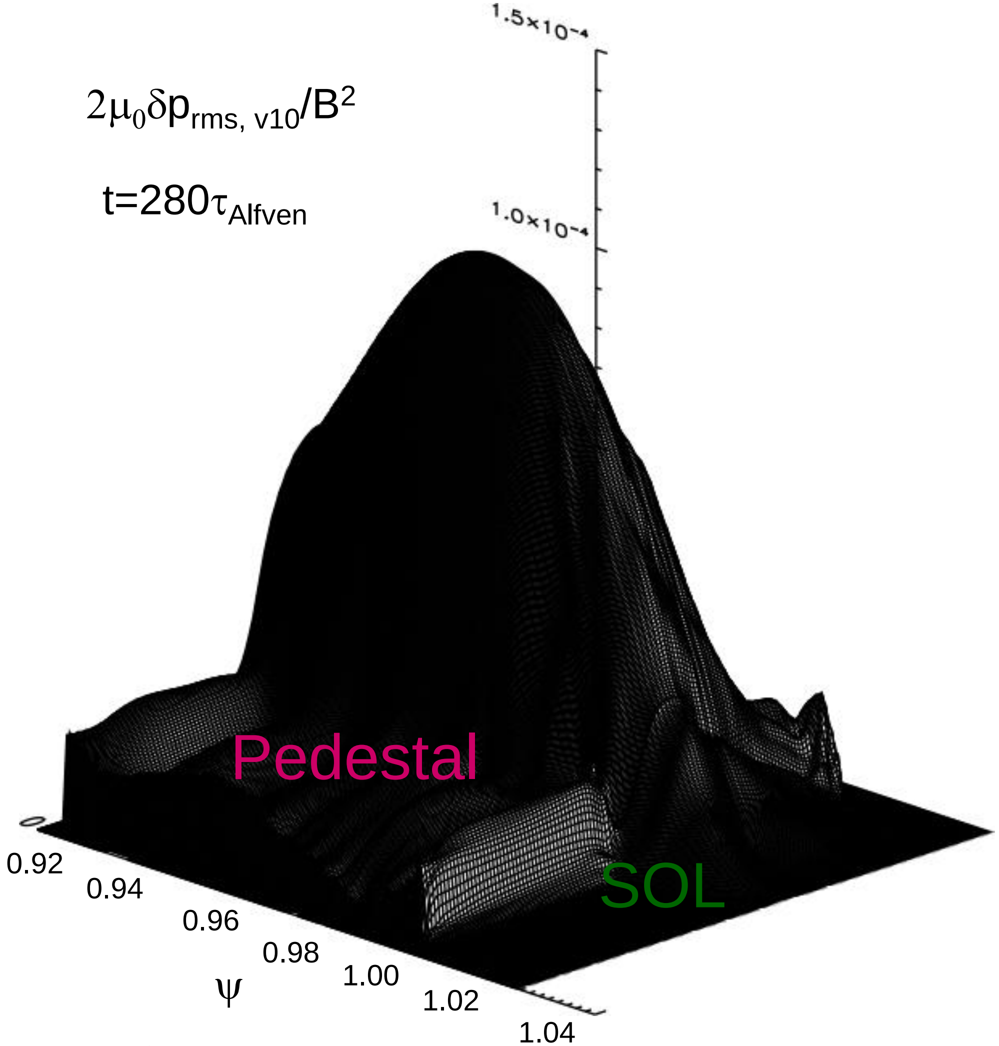

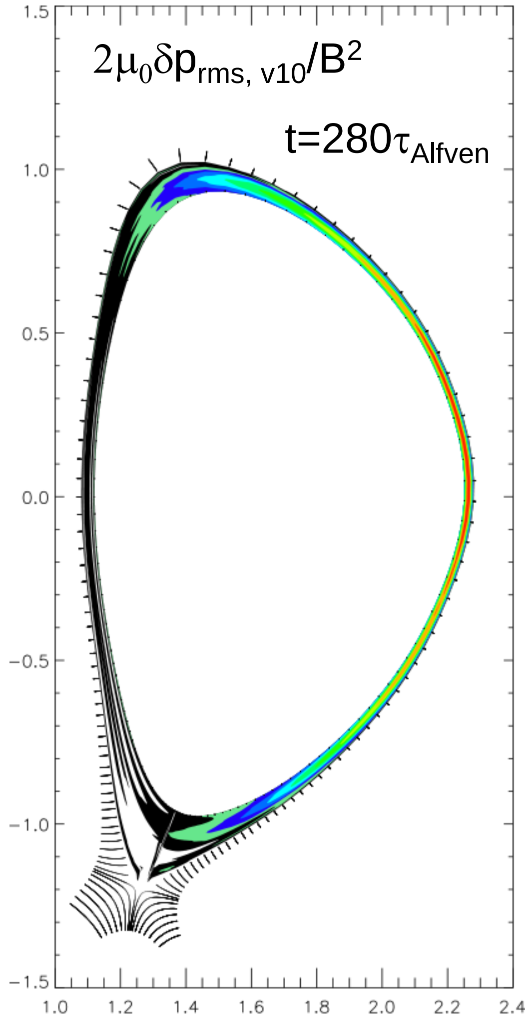

✓X-point magnetic shear limits the poloidal extent of perturbation on low field side.

BOUT++ simulations for one of the latest designs of the ITER 15 MA inductive ELMy H-mode scenario (under the burning condition)

- Simulations starting from equilibrium generated by the CORSICA code.

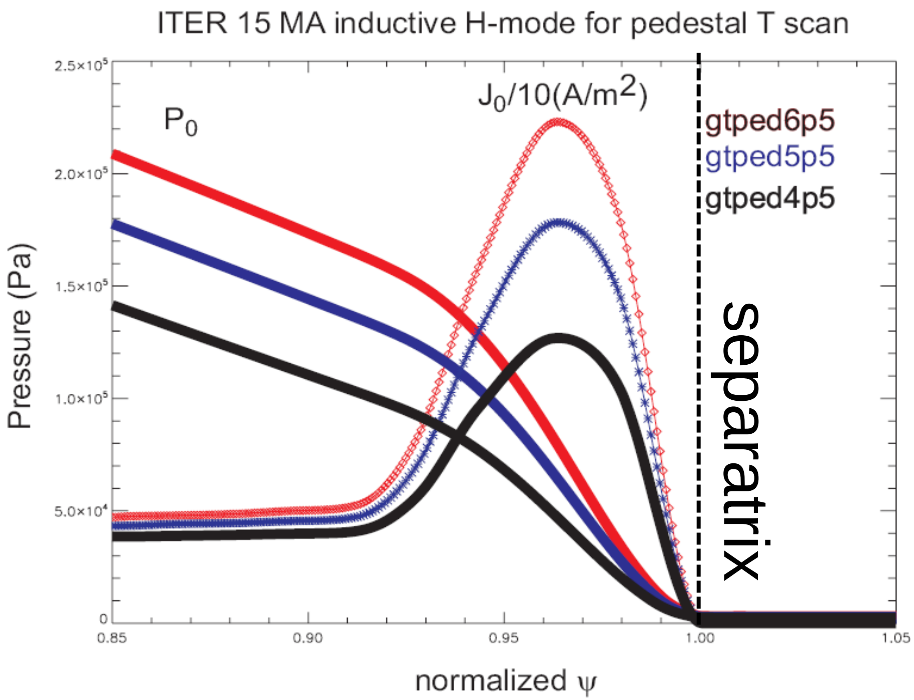

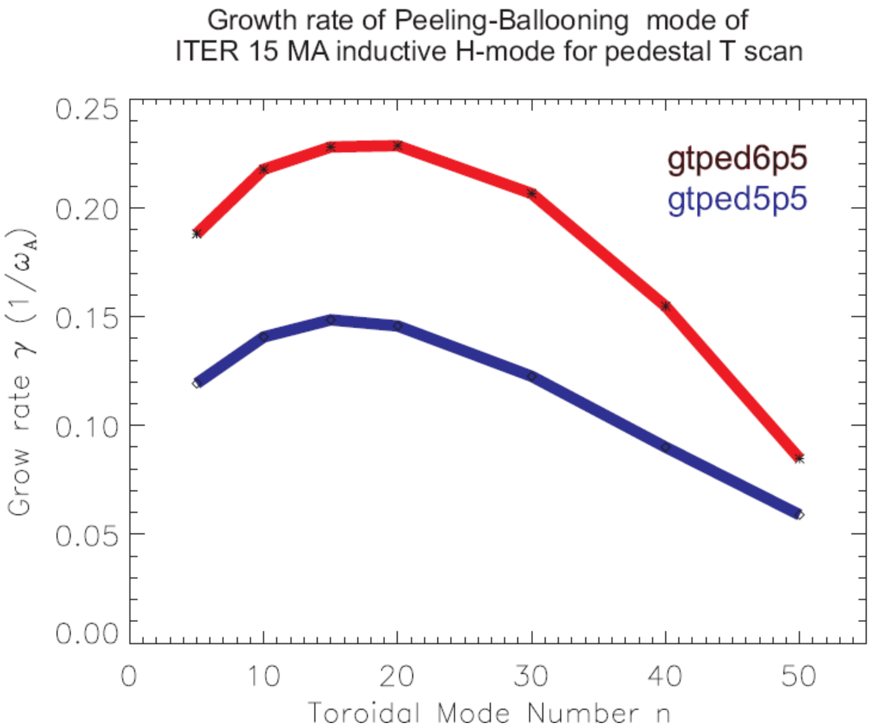

- Marginal unstable pedestal case, T_{ped}=5.5keV, n_{max}=15
- The calculations impact previous ITER ELMy H-mode scenario design as it was based on the pedestal height T_{ped}=4.5keV

X.Q.Xu, B.D.Dudson, P.B.Snyder, M.V.Umansky, H.R.Wilson and T.Casper, Nucl. Fusion 51 (2011)

BOUT++ simulations for one of the latest designs of the ITER 15 MA inductive ELMy H-mode scenario

It is numerical challenge to simulation ITER divertor geometry, requiring high resolutions nx > 1000, ny>100, even for linear mode.

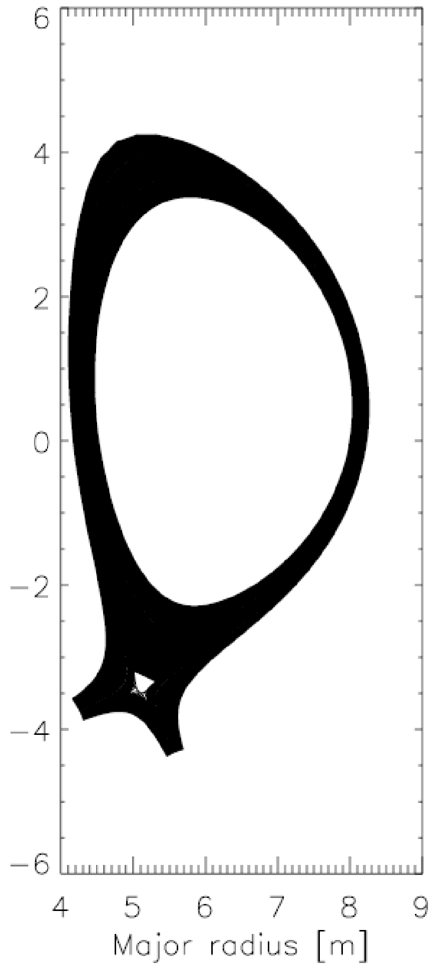

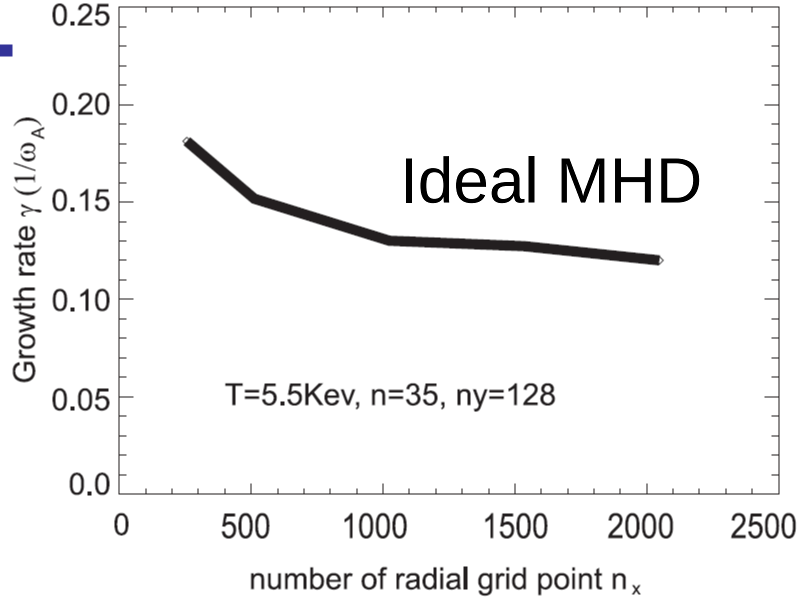

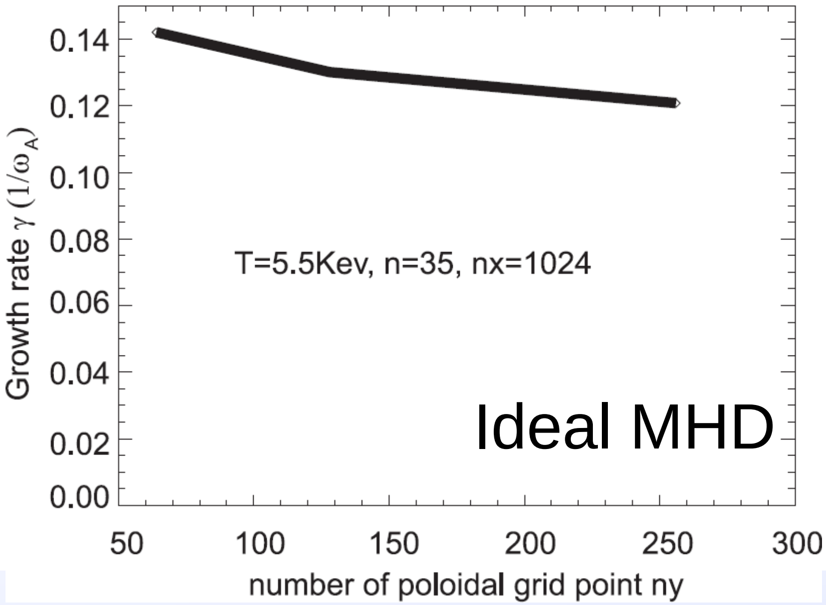

X.Q.Xu, B.D.Dudson, P.B.Snyder, M.V.Umansky, H.R.Wilson and T.Casper, Nucl. Fusion 51 (2011)

BOUT++ simulations show radial and poloidal mode structures and for the ITER 15 MA inductive ELMy H-mode scenario

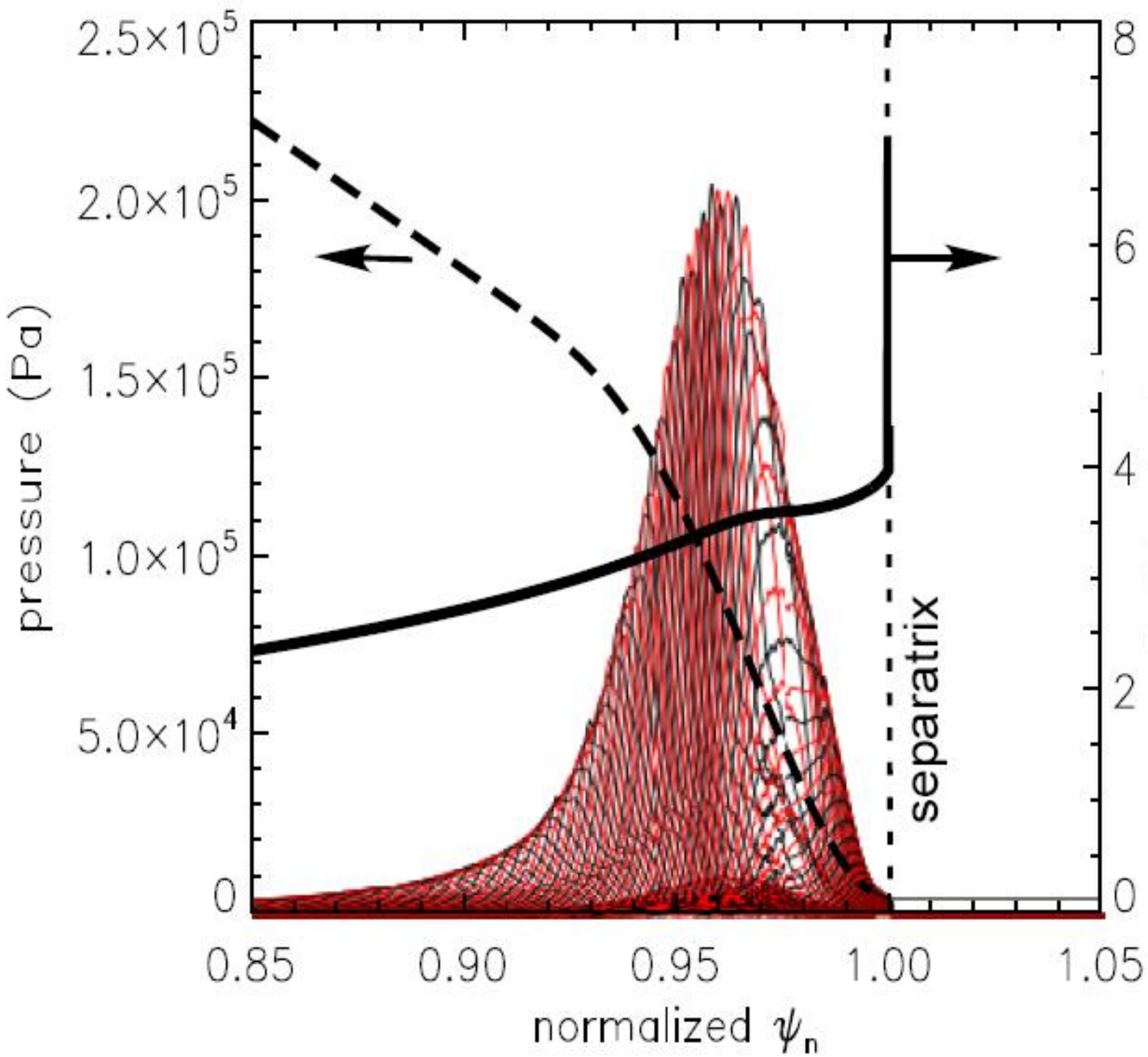

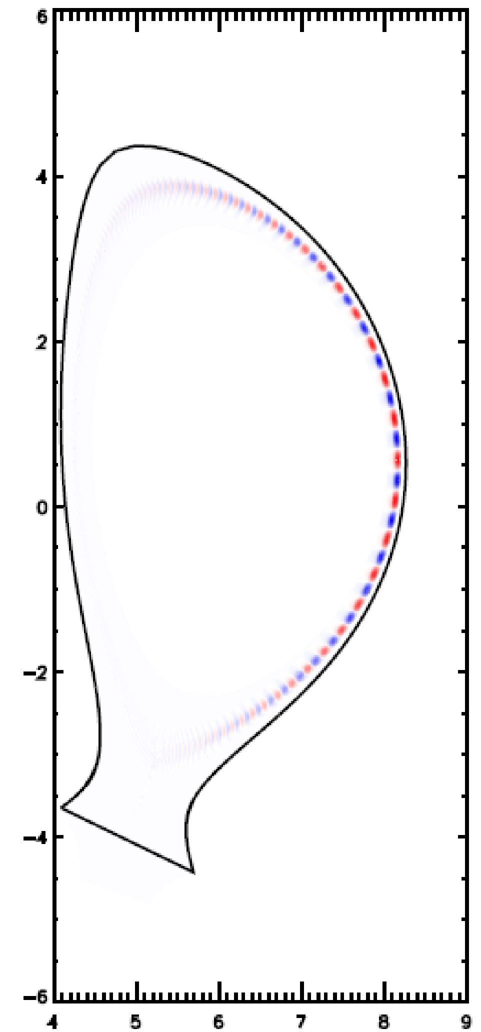

X.Q.Xu, B.D.Dudson, P.B.Snyder, M.V.Umansky, H.R.Wilson and T.Casper, Nucl. Fusion 51 (2011)

BOUT++ Calculations Show NSTX discharge 129032 Resistively Unstable

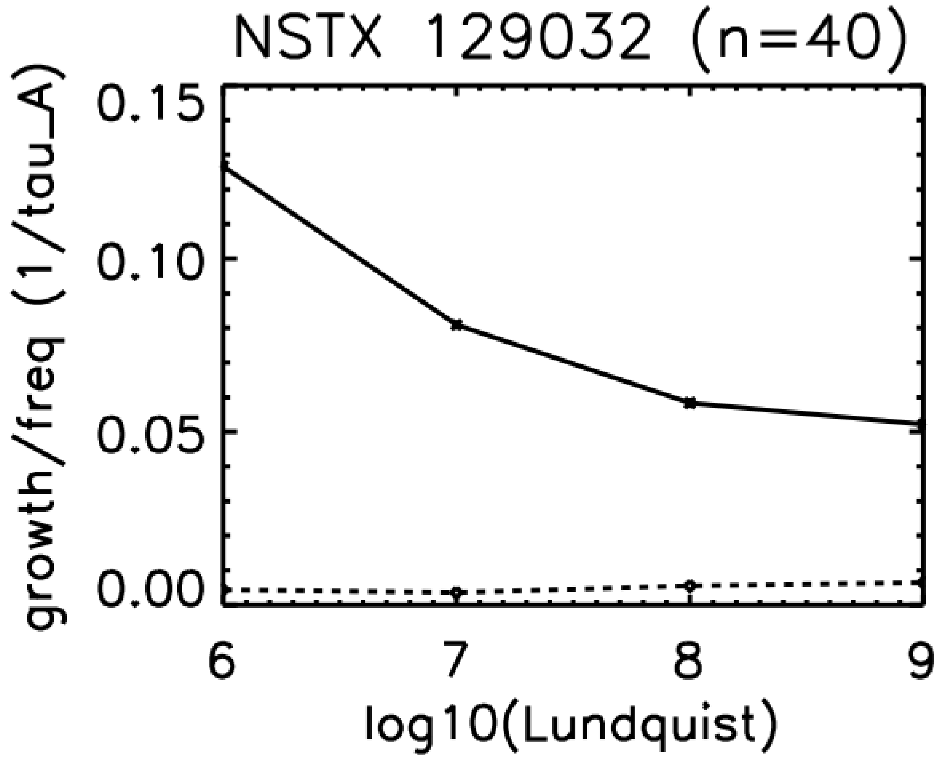

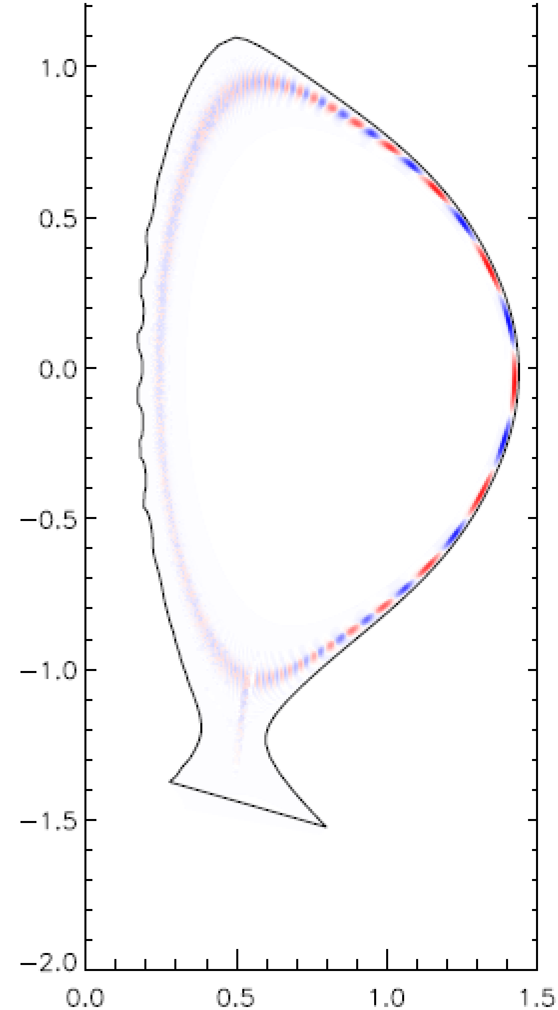

✓With assumption that $V_{ExB}=V_{diam}$, all modes are stabilized.
✓The detailed flow profile does matter for this discharge

Magnetic Reconnection and Pedestal Collapse during ELMs

Equilibrium current and pressure profiles used as BOUT++ input

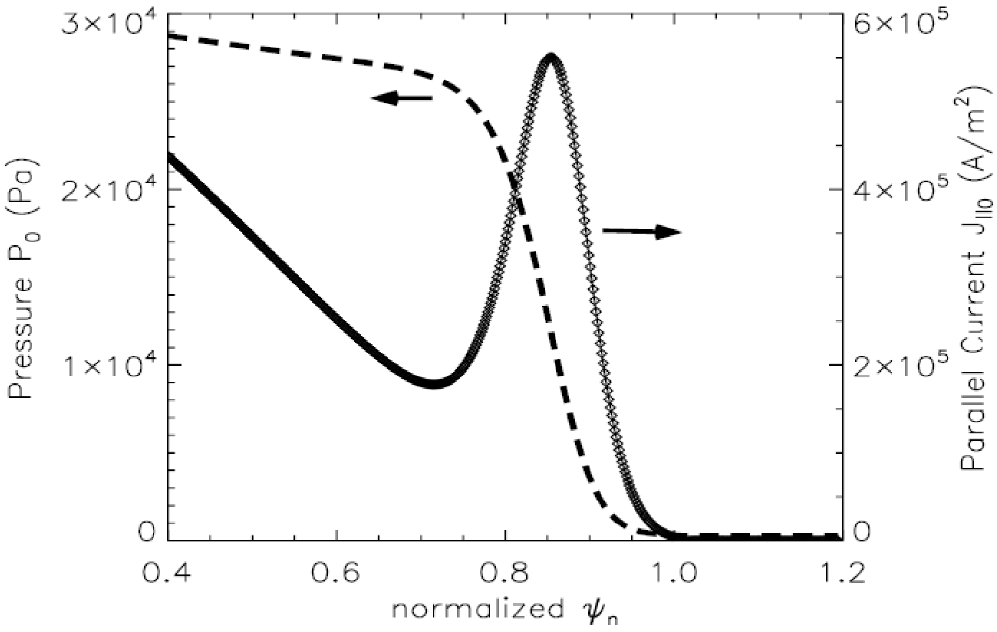

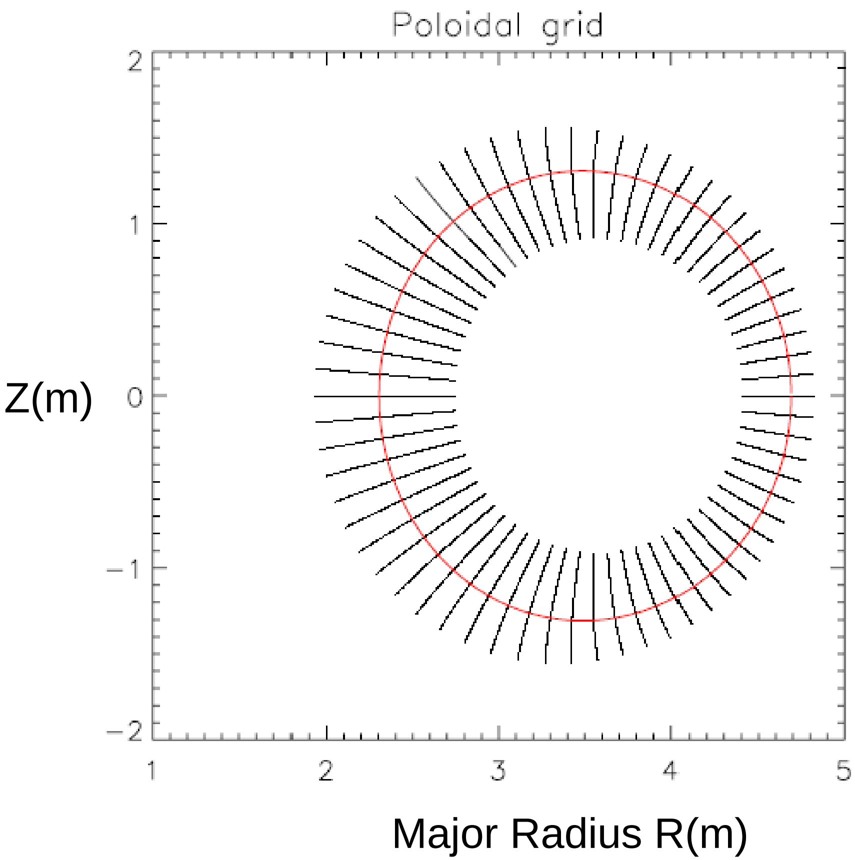

Flux-surface-averaged pressure profile $2m_0 \langle P \rangle / B^2$ vs S with $S_H=10^{12}$

low S -> large ELM size, ELM size is insensitive when $S>10^7$

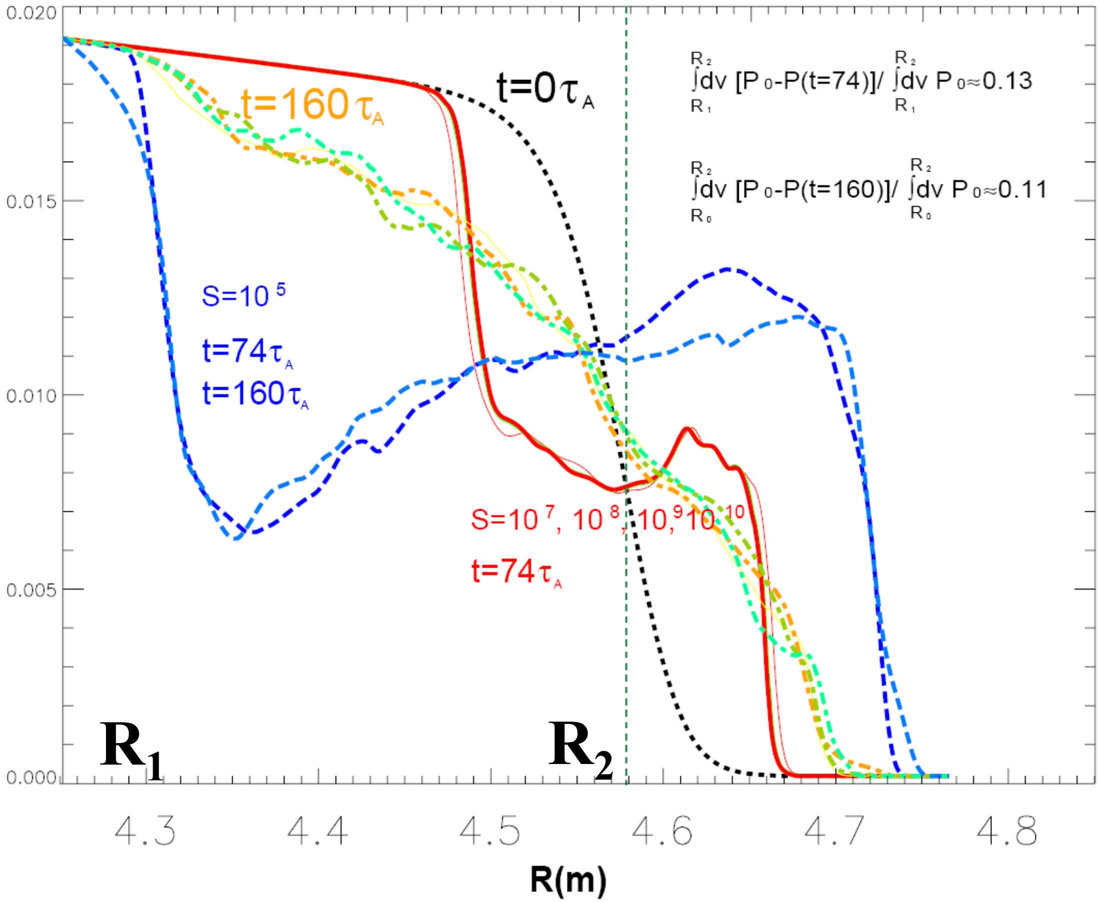

ELM size= $\Delta W_{ped}/ W_{ped}$

ΔW_{ped}= the ELM energy loss

W_{ped} =pedestal stored energy

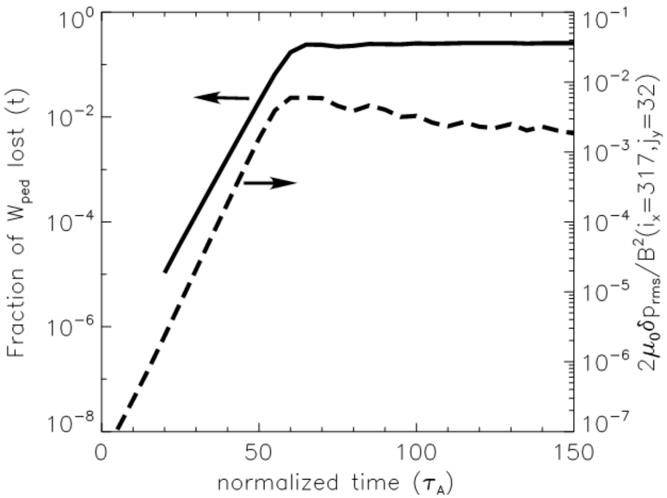

(1) a sudden collapse: P-B modes -> magnetic reconnection -> bursting process

(2) a slow backfill as a turbulence transport process

X.Q.Xu, B.D.Dudson, P.B.Snyder, M.V.Umansky, H.R.Wilson, Phys. Rev. Lett. V105 175005 (2010)

For S=10^8, S_H=10^{12}, the reconnection region is small and the collapse is limited.

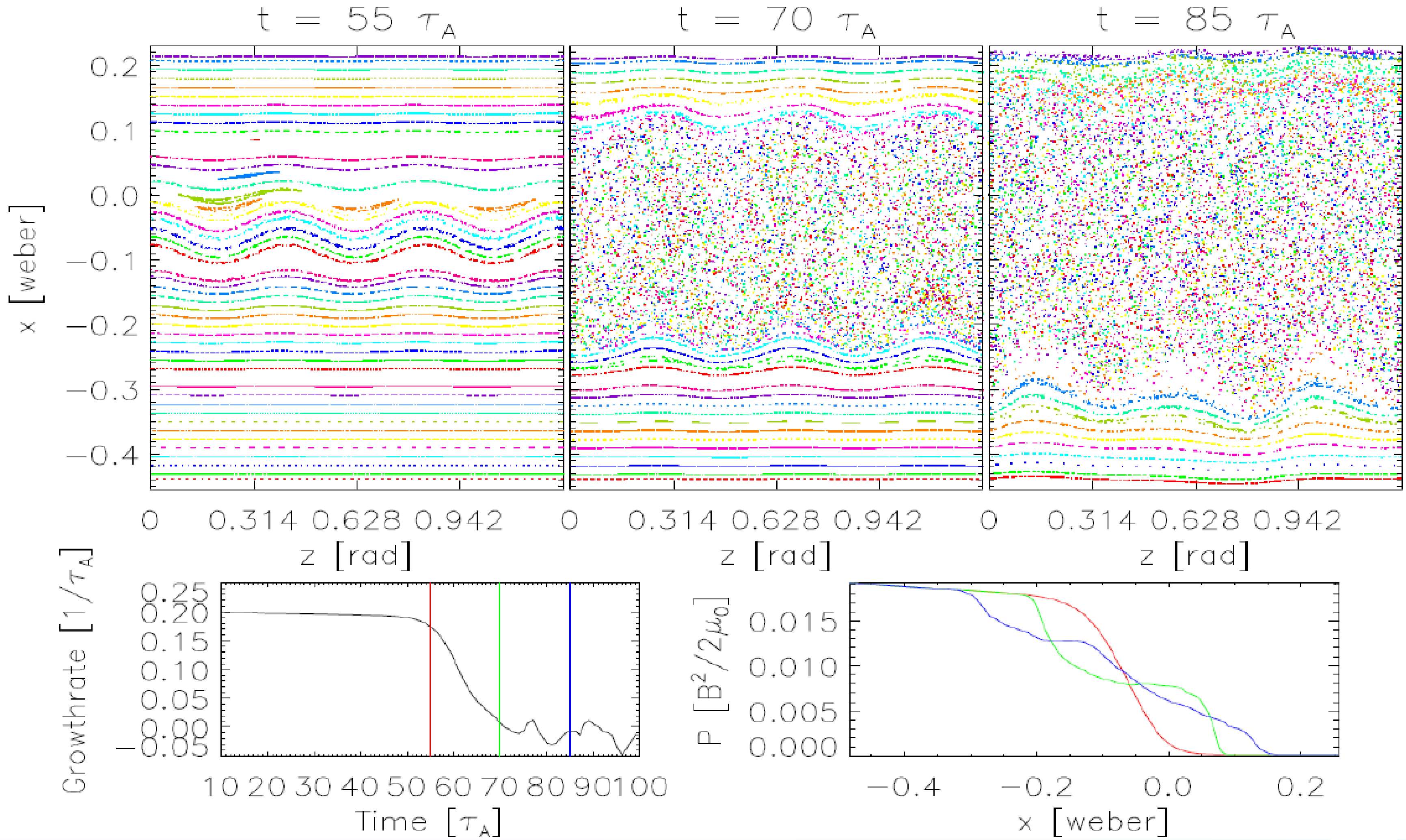

Sauppe, et al, JP9.00098

Role of the hyper-resistivity on nonlinear ELM simulations.

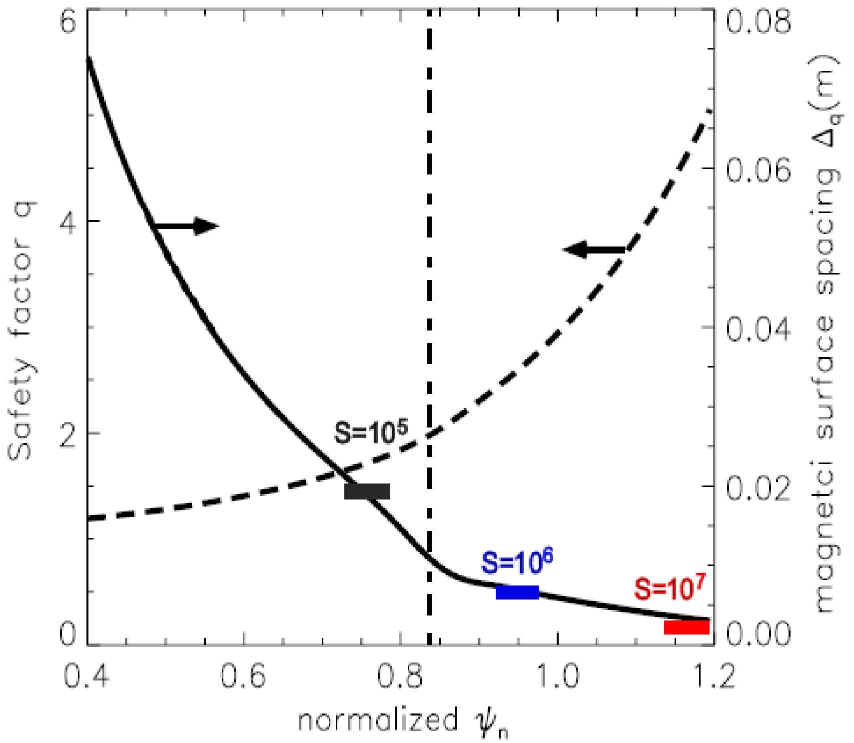

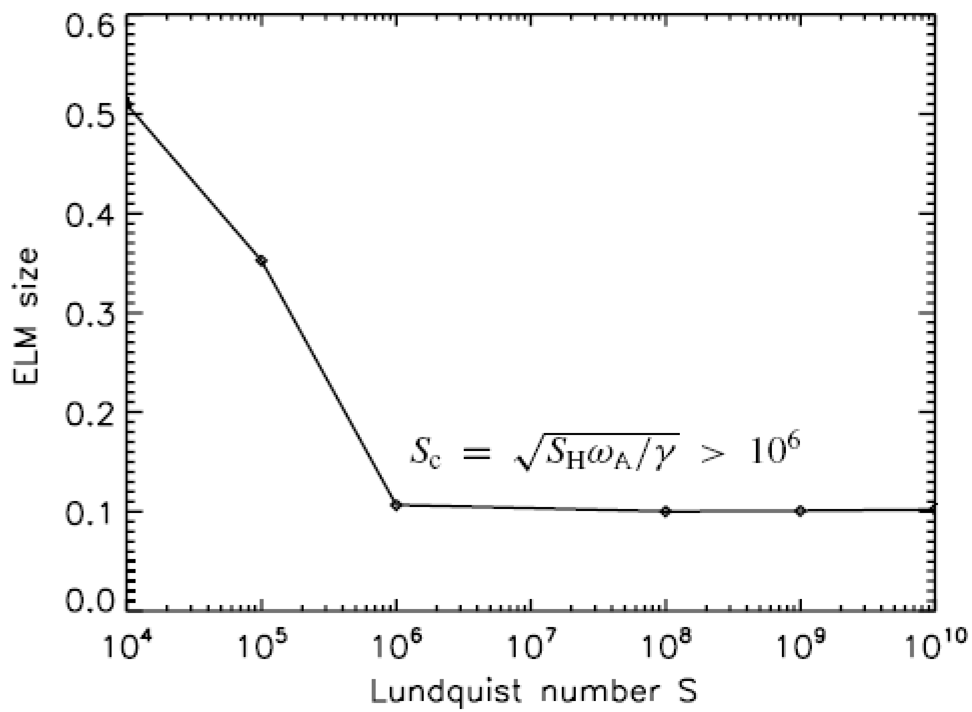

Figure 6. ELM sizes versus Lundquist number S with $S_H = 10^{12}$.

$$\frac{\partial \hat{A}_\parallel}{\partial \hat{t}} = \hat{\nabla}_\parallel \hat{\Phi} + \frac{1}{S} \hat{\nabla}_\perp^2 \hat{A}_\parallel + \frac{1}{S_H} \hat{\nabla}_\perp^4 \hat{A}_\parallel$$

ideal MHD term contains $\nabla_{\parallel 0} = k_\parallel q R_0 = m - nq$

X.Q.Xu, B.D.Dudson, P.B.Snyder, M.V.Umansky, H.R.Wilson and T.Casper, Nucl. Fusion 51 (2011)

Equilibrium flow shear model

$$\frac{\partial \varpi}{\partial t} + \big(\overbrace{\boxed{\underbrace{\mathbf{V}_{EP0}}_{\text{Diamagnetic convection flow}} + \underbrace{\mathbf{V}_{EV0}}_{\text{Net flow}}}}^{\text{Total convection flow}}\big) \cdot \nabla \varpi + \overbrace{\boxed{\mathbf{V}_1 \cdot \nabla \varpi_0}}^{\text{Kelvin-Helmholtz term}} = B_0^2 \nabla_{\parallel} J_{\parallel} + 2\mathbf{b_0} \times \kappa \cdot \nabla P_1$$

$$\varpi = \frac{\rho_0}{B_0}\Big(\nabla_\perp^2 \phi + \overbrace{\frac{1}{n_0 Z_i e} \nabla_\perp^2 P}^{\text{Diamagnetic drift}}\Big)$$

- **Diamagnetic effects:**
  - **Diamagnetic convection flow: EXB** flow that balances diamagnetic flow, is determined by pressure profile, introduces negative electric fi Φ_{dia0} ;
  - **Diamagnetic drift:** inversely depends on density;
- **Net flow:** perpendicular component of toroidal rotation, modeled by a simple function via Φ_{V0} , flexible;
- **Kelvin-Helmholtz term:** curl of net flow, can be switched off;
- **Total convection flow:** flow shear effects come from this total convection flow rather than the net flow.

Equilibrium flow shear can be a double-edged sword on P-B modes

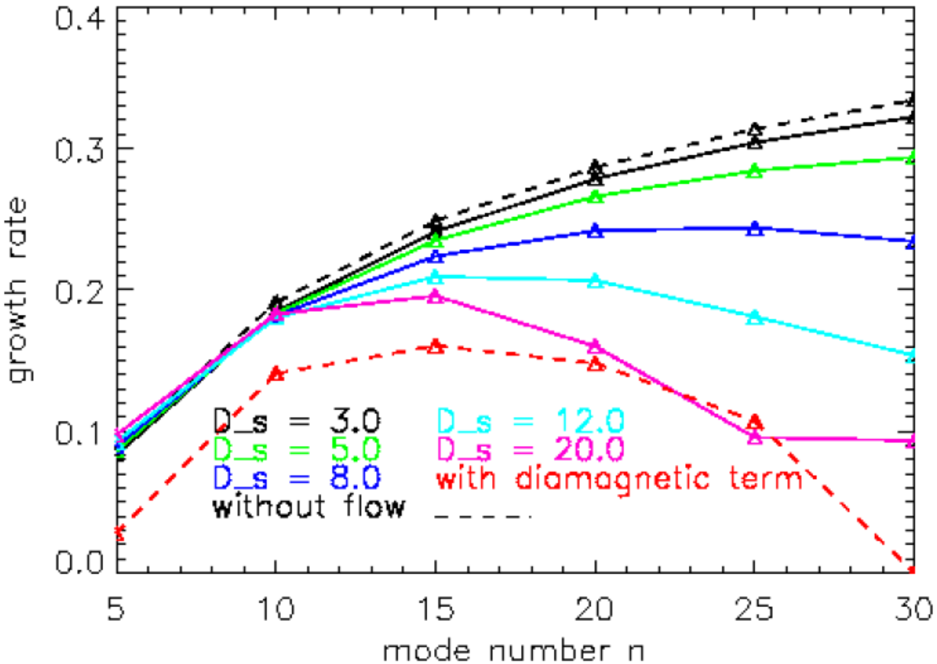

$(\gamma_{KH}-\gamma_{w/o\ KH})/\gamma_{w/o\ KH}$

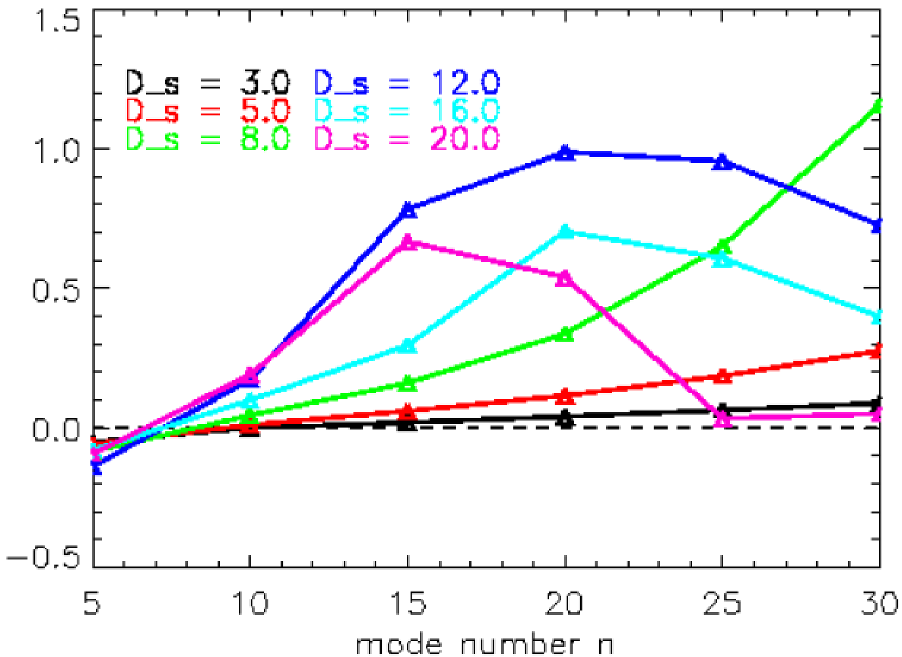

- The flow shear plays the same role as diamagnetic stabilization for ideal MHD case without diamagnetic term.
- Kelvin-Helmholtz drive mainly destabilize intermediate n modes: n=10~30.

5-field Peeling-Ballooning model

- In order to investigate the separate effects of density and temperature effect, we extend the 3-field simple P-B model into 5-field model by separating the total pressure into density electron and temperature

$$\frac{\partial n_i}{\partial t} + \mathbf{V}_E \cdot \nabla n_i = 0,$$

$$\varpi = n_{i0}\frac{m_i}{B_0}\left[\nabla_\perp^2 \phi + \frac{1}{n_{i0}}\boxed{\nabla_\perp \phi \cdot \nabla_\perp n_{i0}} + \frac{1}{n_{i0}Z_i e}\nabla_\perp^2 p\right],$$

$$\frac{\partial T_j}{\partial t} + \mathbf{V}_E \cdot \nabla T_j = 0,$$

$$J_\parallel = J_{\parallel 0} - \frac{1}{\mu_0}\nabla_\perp^2 (B_0 \psi),$$

$$\frac{\partial}{\partial t}\varpi + \mathbf{V}_E \cdot \nabla \varpi = B_0^2 \mathbf{b} \cdot \nabla \frac{J_\parallel}{B_0} + 2\mathbf{b} \times \kappa \cdot \nabla P,$$

$$\mathbf{V}_E = \frac{1}{B_0}\left(\mathbf{b}_0 \times \nabla_\perp \Phi\right),$$

$$P = k_B n (T_i + T_e) = P_0 + p,$$

$$\frac{\partial \psi}{\partial t} = -\frac{1}{B_0}\mathbf{b} \cdot \nabla \Phi + \frac{\eta}{\mu_0}\nabla_\perp^2 \psi - \frac{\eta_H}{\mu_0}\nabla_\perp^4 \psi,$$

$$\Phi = \Phi_0 + \phi.$$

Xia, et al, JP9.00102

The strong stabilizing density effect on P-B modes is due to ion diamagnetic drift

n_0=constant in x, T_{e0} and T_{i0} vary in x

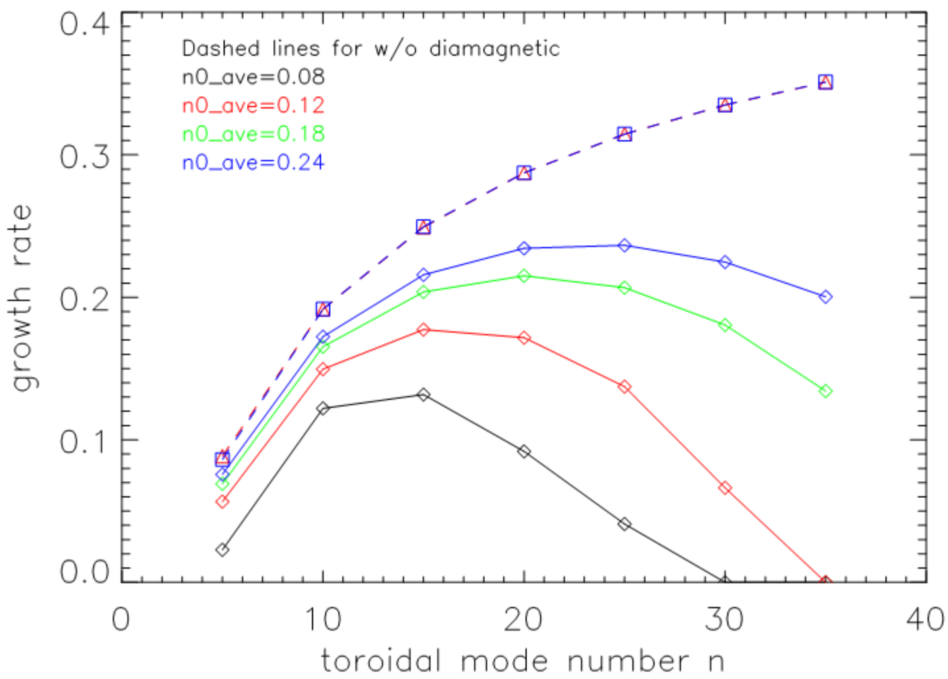

- **For ideal MHD, n_0 does not affects the normalized linear growth rate.**
- **With diamagnetic effects,**
  - **low density results in more stable high-n modes.**

$$n_{i0}(x) = \frac{(n0_{height} \times n_{ped})}{2}\left[1 - \tanh\left(\frac{x - x_{ped}}{\Delta x_{ped}}\right)\right] + n0_{ave} \times n_{ped}\,;$$

Xia, et al, JP9.00102